

POU domain factor *Brn-3b* is required for the development of a large set of retinal ganglion cells

LIN GAN*[†], MENGQING XIANG^{†‡}, LIJUAN ZHOU[‡], DANIEL S. WAGNER*, WILLIAM H. KLEIN*[§],
AND JEREMY NATHANS^{‡¶}

*Department of Biochemistry and Molecular Biology, University of Texas M. D. Anderson Cancer Center, Houston, TX 77030; [‡]Departments of Molecular Biology and Genetics, Neuroscience, and Ophthalmology, Howard Hughes Medical Institute, Johns Hopkins University School of Medicine, Baltimore, MD 21205

Communicated by John W. Littlefield, Johns Hopkins University, Baltimore, MD, January 2, 1996 (received for review October 28, 1995)

ABSTRACT The three members of the *Brn-3* family of POU domain transcription factors are found in highly restricted sets of central nervous system neurons. Within the retina, these factors are present only within subsets of ganglion cells. We show here that in the developing mouse retina, *Brn-3b* protein is first observed in presumptive ganglion cell precursors as they begin to migrate from the zone of dividing neuroblasts to the future ganglion cell layer, and that targeted disruption of the *Brn-3b* gene leads in the homozygous state to a selective loss of 70% of retinal ganglion cells. In *Brn-3b* (–/–) mice other neurons within the retina and brain are minimally or not at all affected. These experiments indicate that *Brn-3b* plays an essential role in the development of specific ganglion cell types.

The retina is a specialized region of the central nervous system with a relatively small number of cell types. Retinal neurons are arranged in three layers: the outer nuclear layer contains photoreceptor cells; the inner nuclear layer contains horizontal, bipolar, and amacrine cells; and the ganglion cell layer contains ganglion cells and displaced amacrine cells. Each of these cell types can be further divided into subtypes that differ in their physiological and morphological properties, and, in the case of ganglion cells, their pattern of central projections. During development, the various retinal neurons are generated by ordered migrations of postmitotic cells from a layer of dividing neuroblasts, a pattern similar to that observed in the generation of cerebral cortical neurons (1–3).

In the mammalian retina there are at least 10 different types of ganglion cells (4, 5). The more common ganglion cell types, especially those with large cell bodies, have been intensively studied. One major group of ganglion cells projects to the lateral geniculate nucleus, forming the first stage of the retinohalamocortical pathway. In primates, where they have been most extensively characterized, these cells are found to have receptive fields that extract information regarding chromatic, spatial, and/or luminance contrast. Most of the remaining ganglion cells project to midbrain targets that control eye and head movements, and many of these cells respond selectively to moving stimuli. In contrast to the current wealth of physiological and anatomical knowledge regarding ganglion cell diversity, we know little about the molecular events that control the arrangement, commitment, and differentiation of these cells.

One approach to understanding neuronal development and diversity begins with a definition of the relevant genetic regulatory events. As a step in this direction, we and others have identified three closely related POU domain genes—*Brn-3a*, *Brn-3b*, and *Brn-3c*—that are expressed in the retina, in the dorsal root and trigeminal ganglia, and in a small number of midbrain nuclei (6–10). (*Brn-3a*, *Brn-3b*, and *Brn-3c* are also

referred to as *Brn-3.0*, *Brn-3.2*, and *Brn-3.1*, respectively, in refs. 8 and 10.) Within the retina, each *Brn-3* gene is expressed exclusively within subsets of ganglion cells (6, 7). The *Brn-3* genes show sequence similarity to the *Caenorhabditis elegans* gene *Unc-86*, which is expressed in a diverse group of neurons and neuronal precursors and is required in a subset of those cells for normal development (11–13). Although the function of the *Brn-3* genes is as yet unknown, their highly localized patterns of expression suggest that they are involved in the development of particular subsets of neurons. In the present work, we test this hypothesis for *Brn-3b* by studying the effects of a targeted disruption of this gene.

MATERIALS AND METHODS

Targeted Disruption of the *Brn-3b* Gene. Mouse *Brn-3b* genomic sequences were isolated from a genomic DNA library (strain 129/J) constructed in λ EMBL3 (14) and using a human *Brn-3b* gene segment as probe (6). To generate the gene targeting construct, the downstream *HindIII* site of the 2.7-kb *BamHI*–*HindIII* fragment 5' to the *Brn-3b* gene was replaced with a *BamHI* site by conversion to a blunt end followed by addition of a *BamHI* linker. The resulting 2.7-kb *BamHI* fragment and the 4.5-kb *HindIII* fragment 3' to the *Brn-3b* gene were inserted in the correct orientation into the *BamHI* and *HindIII* sites in the pNeoTK gene targeting vector (L.G., unpublished work) to create the targeting construct. The targeting construct was linearized at a unique *Not I* site at the edge of the vector, and 25 μ g of linearized DNA was electroporated into 10^7 AB-1 embryonic stem (ES) cells, which were then selected for resistance to G418 and 1-(2-deoxy-2-fluoro- β -D-arabinofuranosyl)-5-iodouracil (FIAU). Among 288 resistant ES colonies, 15 contained the expected homologous recombination event as indicated by Southern blot analysis using flanking probes. Two targeted ES clones, b193 and b230, were injected into C57BL/6J blastocysts to generate chimeric mice, and subsequently the chimeric mice were bred to C57BL/6J mice to produce heterozygous and homozygous mice for further analysis (15). *Brn-3b* (–/–), (+/–), and (+/+) embryos and mice were genotyped by PCR amplification of genomic DNA.

Immunohistochemistry. Immunostaining of dorsal root and trigeminal ganglia, retinal sections, and retinal flat mounts was performed as previously described (6, 7). Antibodies to *Brn-3a*, *Brn-3b*, and *Brn-3c* are described in refs. 6 and 7. Additional antibodies were obtained from the following sources: anti-

Abbreviations: ES, embryonic stem; mAb, monoclonal antibody; CNS, central nervous system; *en*, embryonic day *n*; DAPI, 4',6'-diamidino-2-phenylindole; TUNEL, terminal dUTP nick end labeling.

[†]L.G. and M.X. contributed equally to this work.

[‡]To whom reprint requests should be addressed at: 15151 Holcombe Boulevard, M.D. Anderson Cancer Center, Houston, TX 77030.

[¶]To whom reprint requests should be addressed at: 805 Preclinical Teaching Building, 725 North Wolfe Street, Johns Hopkins University School of Medicine, Baltimore, MD 21205.

The publication costs of this article were defrayed in part by page charge payment. This article must therefore be hereby marked "advertisement" in accordance with 18 U.S.C. §1734 solely to indicate this fact.

Thy-1, Boehringer-Mannheim; SMI-32, Sternberger Monoclonals; and anti-tyrosine hydroxylase and anti-glutamic acid decarboxylase, Chemicon.

Histology and Anatomy. Semithin and ultrathin sections of optic nerves and retinas were prepared as described in ref. 16, with the following modifications. Animals were perfused transcardially with phosphate-buffered saline (PBS) followed by 2% paraformaldehyde and 2% glutaraldehyde in PBS. Tissues were postfixed overnight at 4°C in the same fixative. Following three 10-min rinses in 50 mM sodium cacodylate (pH 7.4), they were postfixed at 4°C for 2 hr in 1% osmium tetroxide in 50 mM sodium cacodylate. The fixed tissues were then rinsed in 50 mM sodium cacodylate, dehydrated in graded ethanol solutions, and infiltrated and embedded in epoxy resin. Semithin sections stained with toluidine blue were examined by light microscopy, and ultrathin sections stained with uranyl acetate, by electron microscopy.

Cresyl violet staining of frozen sections was performed as described in ref. 17. Neuroanatomic assignments were made with reference to refs. 18 and 19. For SYTOX staining, mice were perfused transcardially with PBS followed by 4% paraformaldehyde in PBS. Following enucleation, eyecups were prepared and were postfixed overnight at 4°C in the same fixative. The eyecups were rinsed three times for 5 min in PBS, and stained with 1 μ M SYTOX green fluorescent dead cell stain (Molecular Probes, Inc.) in PBS for 5 hr at room

temperature. After three 10-min washes with PBS, the whole-mount retinas were peeled off and mounted on gelatin-coated microslides with the ganglion cell layer facing up. The density of stained nuclei within the ganglion cell layer was determined in the vicinity of the optic disc, where the density of these cells changes little with direction or eccentricity (20). Due to the high density of cells within the inner and outer nuclear layers, cell counts for these layers were obtained from 1- μ m plastic sections rather than from retina whole mounts.

RESULTS AND DISCUSSION

Phenotype of *Brn-3b* (-/-) Mice. To determine the role of *Brn-3b* *in vivo*, mice lacking the *Brn-3b* gene were generated by homologous recombination in ES cells (Fig. 1). Mice that are either homozygous or heterozygous for the mutant allele [*Brn-3b* (-/-) or (+/-), respectively] are indistinguishable from their wild-type [(+/+)] littermates in viability, growth rate, fertility, gait, and response to handling. These characteristics suggest that in *Brn-3b* (-/-) and (+/-) mice the somatosensory and motor systems are grossly intact. Visual system function is more difficult to assess by inspection, as bilateral enucleation or hereditary retinal degeneration does not produce a noticeable difference in the above characteristics.

Consistent with the inferred normality of somatosensory function, the trigeminal and dorsal root ganglia, which repre-

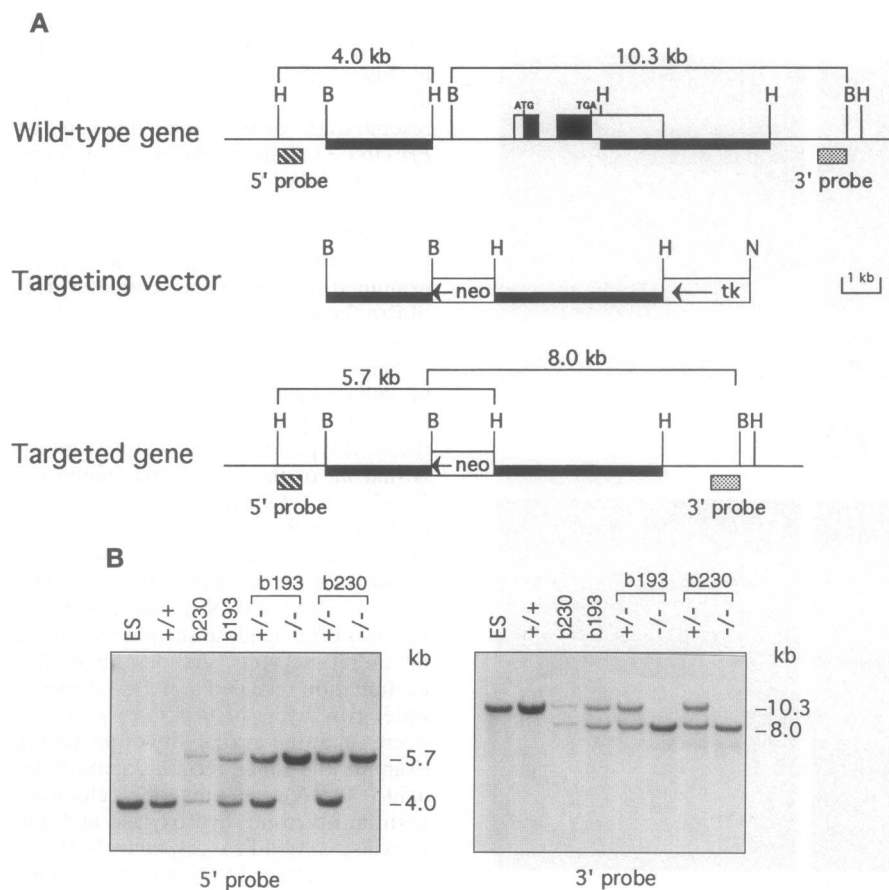


FIG. 1. Targeted disruption of the *Brn-3b* gene. (A) Restriction maps of the mouse *Brn-3b* gene, the targeting construct, and the predicted structure of the targeted *Brn-3b* allele. The two exons are shown as boxes, with the open portion indicating the 5' and 3' untranslated regions and the filled portions indicating the protein coding regions. In the targeting construct, a 4.4-kb segment encompassing the complete *Brn-3b* coding region was replaced with a PGK-neo cassette (neo), which was flanked by 2.7 kb of *Brn-3b* 5' and 4.5 kb of *Brn-3b* 3' sequences (thick black lines). An MC1-tk cassette (tk) was added for negative selection. The orientations of the PGK-neo and MC1-tk cassettes are indicated by arrows. Also indicated are the sizes of the expected wild-type and targeted *Hind*III and *Bam*HI fragments detected by using an external 5' probe (0.5-kb *Hind*III-*Sma* I fragment; striped box) and an external 3' probe (0.7-kb *Sma* I-*Bam*HI fragment; shaded box). Restriction enzyme sites: B, *Bam*HI; H, *Hind*III; N, *Not* I. (B) Southern blot analysis of two targeted ES cell lines, b193 and b230, and tail DNA isolated from pups from the two resulting mouse lines. The 5' probe identifies 4.0-kb wild-type and 5.7-kb targeted *Hind*III fragments, and the 3' probe identifies 10.3-kb wild-type and 8.0-kb targeted *Bam*HI fragments. ES, AB1 ES cells; +/+, wild type; +/-, heterozygote; -/-, homozygous mutant.

sent two principal sites of *Brn-3b* expression, appeared indistinguishable between *Brn-3b* ($-/-$) and ($+/+$) mice at the light microscopic level. Immunostaining of these ganglia with antibodies against Brn-3a, Brn-3b, and Brn-3c (6, 7) revealed the expected absence of Brn-3b immunoreactivity but no alteration in the pattern or abundance of neurons expressing *Brn-3a* or *Brn-3c* (data not shown).

Retinal Ganglion Cell Defects. In contrast to the trigeminal and dorsal root ganglia, specific defects were found within the retinas of *Brn-3b* ($-/-$) mice. While the overall structure of the *Brn-3b* ($-/-$) retina resembles that of the wild type, retinas from *Brn-3b* ($-/-$) mice are on average 20% thinner, due primarily to a decrease in the thickness of the inner plexiform, ganglion cell, and nerve fiber layers. Quantitation of the number of nuclei in each of the retinal layers shows reductions of 30%, 15%, and 10% in the ganglion cell layer, the inner nuclear layer, and the outer nuclear layer, respectively (Figs. 2 and 3 *A* and *B*).

In the ganglion cell layer of both mouse and rat retinas, displaced amacrine cells and ganglion cells each constitute approximately one-half of the cells (20, 21). As one approach to determining which of these cell types is underrepresented in *Brn-3b* ($-/-$) retinas, we immunostained retinas with anti-Thy-1, which stains the axons and dendrites of all ganglion cells (22), and with mAb SMI-32, which predominantly labels the axons of large ganglion cells (23). As seen in Fig. 3 *C-F*, *Brn-3b* ($-/-$) mice show a large reduction in both Thy-1 and SMI-32

immunoreactive processes, suggesting a significant loss of retinal ganglion cells. To characterize the retinal ganglion cells that remain in the *Brn-3b* ($-/-$) retina, we examined the distribution within the retina of Brn-3a and Brn-3c proteins, as these are specific markers for ganglion cells. In the wild-type mouse retina, 35% of cells within the ganglion cell layer contain Brn-3a and Brn-3b, and 15% contain Brn-3c (7); Brn-3a and Brn-3b proteins are therefore present in approximately 70% and Brn-3c in approximately 30% of ganglion cells. Double immunolabeling experiments show that the cells expressing Brn-3a and Brn-3b are largely coincident, and that most of the cells expressing *Brn-3c* also express *Brn-3a* and *Brn-3b* (7). As seen in Fig. 3 *G-L*, in the *Brn-3b* ($-/-$) retina, Brn-3b immunoreactivity is absent as expected, and the number of cells containing Brn-3a and Brn-3c is reduced to approximately 15% of the wild-type number. The cells containing Brn-3a and Brn-3c that are present in the *Brn-3b* ($-/-$) retina may represent a subpopulation of ganglion cells that do not normally express *Brn-3b*.

Optic Nerve Defects. Each retinal ganglion cell gives rise to a single axon which exits the eye as part of the optic nerve. We therefore examined the optic nerves in *Brn-3b* ($-/-$) and ($+/+$) littermates as an independent measure of ganglion cell number and viability. *Brn-3b* ($-/-$) mice show a striking reduction in optic nerve diameter that is apparent to the unaided eye (Fig. 4*A*). Cross sections of optic nerve show an average reduction of 5-fold in the cross-sectional area in *Brn-3b* ($-/-$) mice compared with their wild-type littermates ($n = 4$) with a range of 3- to 7-fold (Fig. 4 *B* and *C*). As seen in Fig. 4 *D* and *E*, *Brn-3b* ($-/-$) optic nerves show a distribution of axon diameters and myelination that closely resembles the distribution in the *Brn-3b* ($+/+$) control, but the *Brn-3b* ($-/-$) nerve differs in having a 1.5-fold lower density of axons. All of the experiments described above were carried out with the *Brn-3b* mutant line b230 (Fig. 1); homozygous mutant animals from a second independently derived *Brn-3b* ($-/-$) line (b193; Fig. 1) showed the same defects when examined for optic nerve diameter, retinal thickness, number of Brn-3a-immunoreactive cells, and anti-Thy-1 stained retinal axons.

These data indicate that *Brn-3b* ($-/-$) retinas have a 60–80% reduction in the number of ganglion cells. Since *Brn-3b* is expressed in approximately 70% of ganglion cells in the wild-type retina, the simplest interpretation of these data is that all of the *Brn-3b*-expressing cells are missing. In the *Brn-3b* ($-/-$) retina, the subset of ganglion cells that remain and express *Brn-3a* and/or *Brn-3c* is likely to be the source of most or all of the remaining axons within the optic nerve.

Analysis of the Inner Retina and Brain. In the central nervous system (CNS), the absence of one population of neurons often leads to secondary losses in populations of input or target neurons. As described above, light microscopic examination revealed a modest decrease in cell number in the outer two layers of *Brn-3b* ($-/-$) retinas, perhaps due to a decrease in the availability of postsynaptic targets. To further examine the inner retina, dopaminergic and γ -aminobutyric acid (GABA)ergic amacrine cells were selectively visualized with anti-tyrosine hydroxylase and anti-glutamic acid decarboxylase antibodies, respectively (Fig. 5). In contrast to the marked decrease in the number of ganglion cells, the number of tyrosine hydroxylase-immunoreactive amacrine cells appears similar in *Brn-3b* ($-/-$) and *Brn-3b* ($+/+$) retinas. Similarly, glutamic acid decarboxylase immunostaining suggests that a large number of GABAergic amacrine cells are present in both *Brn-3b* ($-/-$) and *Brn-3b* ($+/+$) retinas, although individual GABAergic amacrine cells could not be clearly resolved due to their high density and broad arborization. The principal targets of retinal ganglion cell innervation within the brain, the lateral geniculate nucleus, and the superior colliculus were examined by cresyl violet staining of

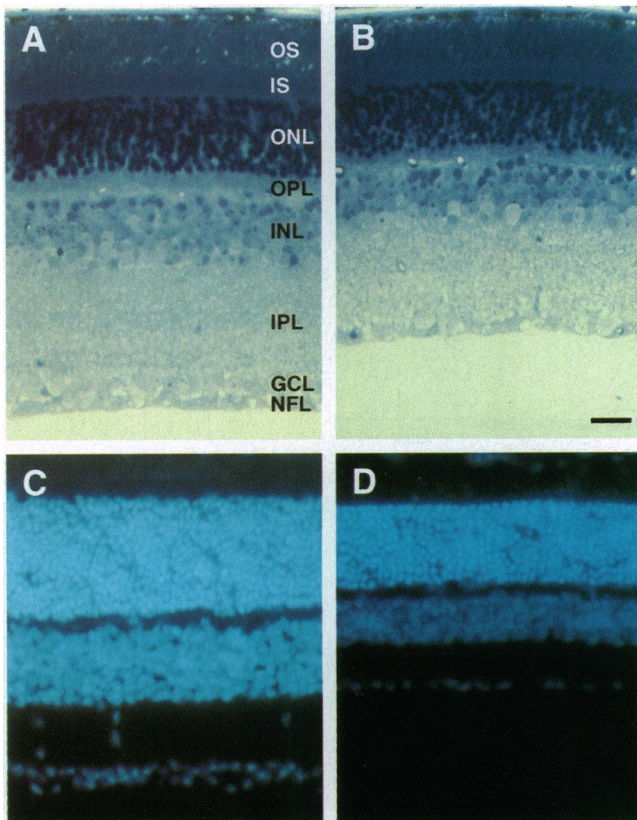


FIG. 2. Retinal structure in *Brn-3b* ($+/+$) and *Brn-3b* ($-/-$) mice. (*A* and *B*) Plastic-embedded 1- μ m sections of *Brn-3b* ($+/+$) (*A*) or *Brn-3b* ($-/-$) (*B*) retinas stained with toluidine blue. (*C* and *D*) 4',6-Diamidino-2-phenylindole (DAPI) staining to visualize nuclei in 10- μ m sections of *Brn-3b* ($+/+$) (*C*) or *Brn-3b* ($-/-$) (*D*) retinas. In this figure and in Figs. 3–5, paired samples were obtained from adult littermates. In these and all other figures the outer nuclear layer is at the top. OS, outer segments; IS, inner segments; ONL, outer nuclear layer; OPL, outer plexiform layer; INL, inner nuclear layer; IPL, inner plexiform layer; GCL, ganglion cell layer; NFL, nerve fiber layer. (The bar in *B* represents 25 μ m; magnification of *A–D*, $\times 260$.)

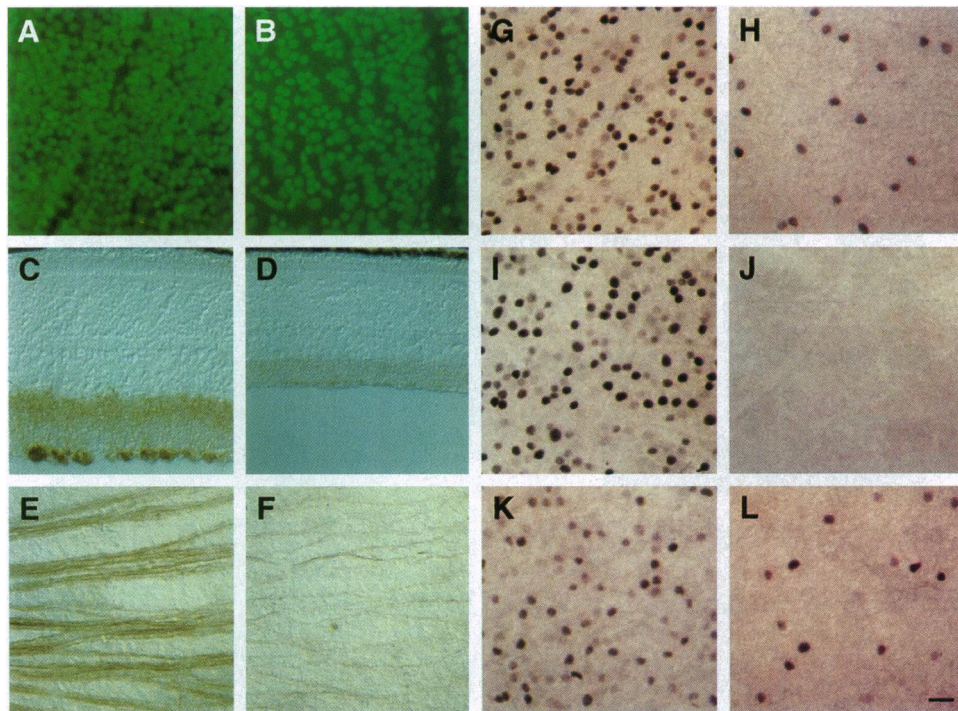


FIG. 3. Reduction in the number of retinal ganglion cells in *Brn-3b* ($-/-$) mice. For each pair of micrographs, a *Brn-3b* ($+/+$) retina is on the left and a *Brn-3b* ($-/-$) retina is on the right. (A and B) Retinal whole mounts in which nuclei are visualized by staining with SYTOX; the region shown is in the vicinity of the optic disc and the plane of focus is in the ganglion cell layer. (C and D) Sections ($10\ \mu\text{m}$) immunostained with anti-Thy-1 monoclonal antibody (mAb). (E and F) Retinal whole mounts immunostained with mAb SMI-32, a marker for large ganglion cells and their axons. (G-L) Retinal whole mounts immunostained with affinity-purified anti-Brn-3a (G and H), anti-Brn-3b (I and J), or anti-Brn-3c (K and L). As described previously (2), the abundance of the Brn-3 proteins shows a characteristic heterogeneity among different cells. (The bar in L represents $25\ \mu\text{m}$; magnification of A-L, $\times 260$.)

coronal sections from adult *Brn-3b* ($-/-$) and ($+/+$) littermates (data not shown). The size and cellularity of both the lateral geniculate nucleus and the superior colliculus appear to be unaffected in *Brn-3b* ($-/-$) mice, suggesting that the remaining retinal ganglion cells may provide sufficient innervation to maintain the viability of most or all neurons within these regions.

Brn-3b in the Developing Retina. The retinal ganglion cell defects present in *Brn-3b* ($-/-$) mice indicate that Brn-3b plays a critical role in the development of these cells. If this role includes initiating the program of ganglion cell differentiation, then Brn-3b protein should be present in developing ganglion cells at or prior to the time of this decision. In the mouse, [^3H]thymidine labeling studies show that between embryonic days 11 and 18 (e11 and e18) most ganglion cell precursors become postmitotic and migrate to the future ganglion cell layer at the inner surface of the developing retina (1-3, 24). In the developing chicken retina, immunostaining with a ganglion cell-specific mAb demonstrates that ganglion cells begin to differentiate shortly after their terminal mitosis while they are still migrating (25, 26). Immunostaining of the developing mouse retina shows a progressive increase over time in the number of cells containing Brn-3b in the future ganglion cell layer (Fig. 6). In the mitotic zone, cells containing Brn-3b first appear at e11, and their numbers increase to a peak at approximately e12-e15, corresponding to the time during which the greatest number of ganglion cells are undergoing their final mitoses and are migrating from this zone. These immunostained cells are likely to represent recently postmitotic ganglion cells en route to the ganglion cell layer, suggesting that Brn-3b acts in the earliest steps in ganglion cell differentiation.

The diminution in ganglion cell number observed in adult *Brn-3b* ($-/-$) retinas could reflect either a failure to generate these cells in the developing retina or a failure of these cells to

follow the ganglion cell differentiation program. In the latter case, the affected cells might either die or develop into other retinal cell types. To examine these alternate possibilities, developing *Brn-3b* ($-/-$) and ($+/+$) retinas were examined for the presence of the ganglion cell-specific markers Brn-3a and Brn-3c and for evidence of cell death. Immunostaining of *Brn-3b* ($-/-$) and ($+/+$) retinas at e13.5, e15.5, e16.5, and P1.5 revealed similar time courses of appearance of Brn-3a and Brn-3c, both of which begin to accumulate at e13.5 (M.X. and J.N., unpublished observations). However, at each time point the *Brn-3b* ($-/-$) retinas differ from the ($+/+$) controls in showing approximately 1/5 as many immunostained cells. These data indicate that the reduction in ganglion cell number in *Brn-3b* ($-/-$) mice is evident at a very early stage in ganglion cell development. To quantitate the number and location of dying cells, e13.5 and e15.5 retinas were examined following either *in situ* terminal deoxynucleotidyltransferase (TdT) labeling of fragmented DNA [terminal dUTP nick end labeling (TUNEL) (27)] or DAPI staining. At e13.5 and e15.5, TUNEL labeling revealed, respectively, an average of 2-3 and 8-9 labeled cells per $10\text{-}\mu\text{m}$ retinal section; no difference was observed between *Brn-3b* ($-/-$) and ($+/+$) retinas. By DAPI staining, fragmented and/or homogeneously stained nuclei were observed at a frequency of fewer than 1 per $10\text{-}\mu\text{m}$ section in e13.5 retinas from either *Brn-3b* ($-/-$) or *Brn-3b* ($+/+$) animals. At e15.5, *Brn-3b* ($+/+$) and ($-/-$) retinas showed, respectively, an average of 5 and 14 fragmented and/or homogeneously stained nuclei per $10\text{-}\mu\text{m}$ section, and most of these were localized to the inner part of the dividing neuroblast layer.

These data indicate that at the peak of ganglion cell genesis (e11-e18), when the number of developing ganglion cells in *Brn-3b* ($-/-$) retinas is already greatly reduced, there is little or no increase in cell death in the ganglion cell layer. While the DAPI analysis suggests that in the developing *Brn-3b* ($-/-$)

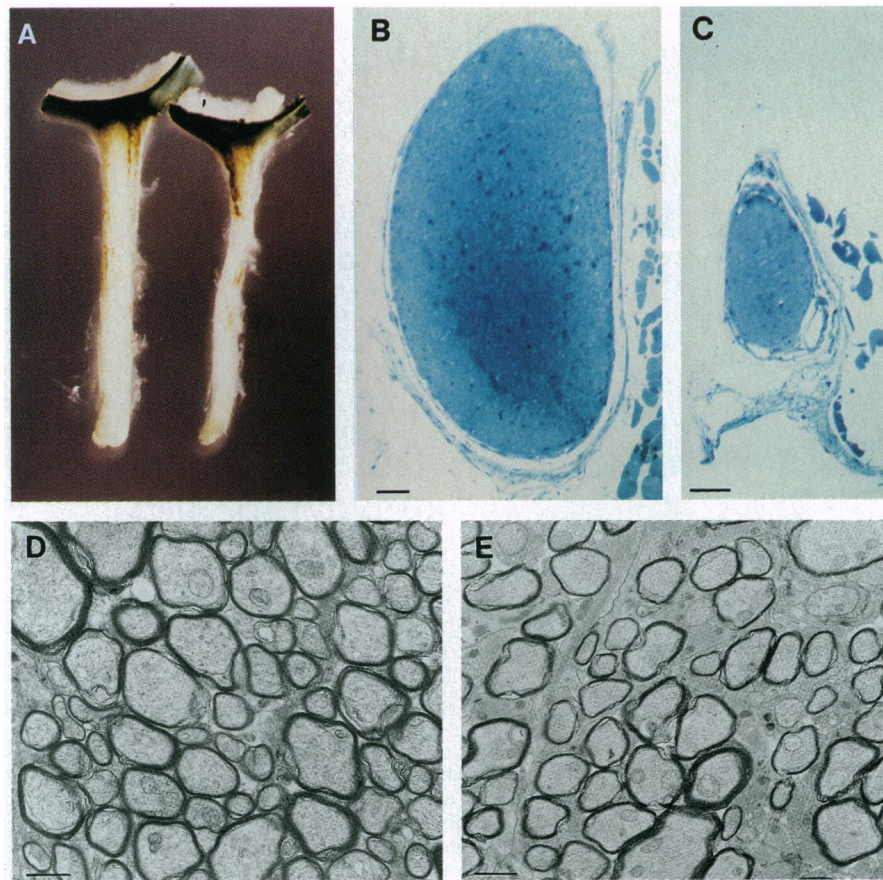


FIG. 4. Reduction in the number of optic nerve fibers in *Brn-3b* ($-/-$) mice. (A) Optic nerve diameter is reduced in a *Brn-3b* ($-/-$) mouse (right) compared with a *Brn-3b* ($+/+$) littermate (left); a small segment of each eye is at the top. (B and C) Plastic-embedded 1- μ m sections through *Brn-3b* ($+/+$) (B) or *Brn-3b* ($-/-$) (C) optic nerves stained with toluidine blue. (D and E) Representative electron micrographs of *Brn-3b* ($+/+$) (D) or *Brn-3b* ($-/-$) (E) optic nerves. (The bars in B and C represent 50 μ m; bars in D and E represent 1 μ m; magnifications: A, $\times 12$; B and C, $\times 120$; D and E, $\times 2900$.)

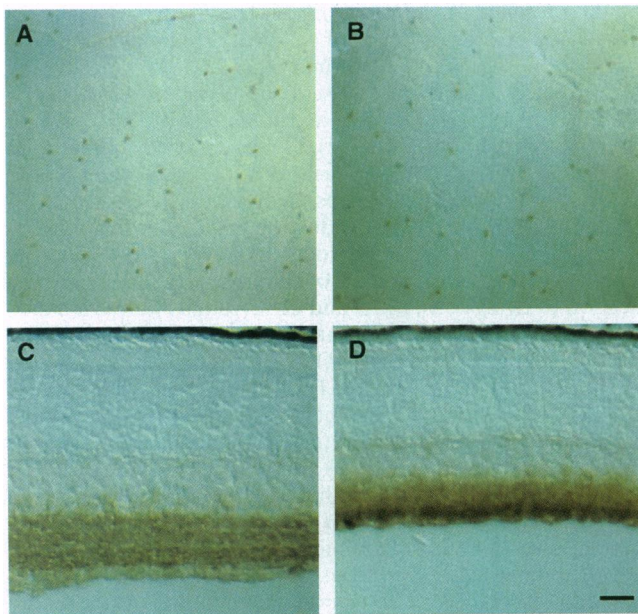


FIG. 5. Density of amacrine cell subsets in *Brn-3b* ($-/-$) mice. (A and B) Amacrine cells containing tyrosine hydroxylase were visualized by retinal whole-mount immunostaining of retinas from *Brn-3b* ($+/+$) (A) or *Brn-3b* ($-/-$) (B) littermates. (C and D) Amacrine cells containing glutamic acid decarboxylase were visualized in 10- μ m sections of retinas from *Brn-3b* ($+/+$) (C) or *Brn-3b* ($-/-$) (D) littermates. (The bar in D represents 25 μ m; magnifications: A and B, $\times 60$; C and D, $\times 230$.)

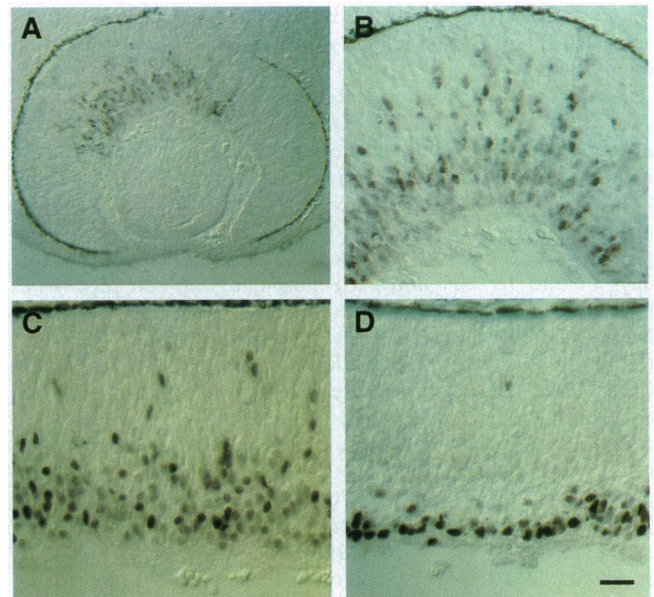


FIG. 6. *Brn-3b* appears early in ganglion cell development. Sections through the developing mouse retina at e12.5 (A), e13.5 (B), e16.5 (C), and P1.5 (D) were immunostained with anti-*Brn-3b*. *Brn-3b* is initially present in both the developing ganglion cell layer and the proximal part of the mitotic zone; as development proceeds *Brn-3b* is increasingly confined to cells within the developing ganglion cell layer. The localized expression of *Brn-3b* within the central retina at e12.5 reflects the earlier development of the central retina. (The bar in D represents 25 μ m; magnifications: A, $\times 120$; B, C, and D, $\times 230$.)

retina there may be an increase in cell death in the inner nuclear layer, we have no evidence for differential cell death by TUNEL staining. These results suggest that in the absence of Brn-3b the affected ganglion cell precursors fail to appear during development and that the modest reduction in cell number in the inner and outer nuclear layers of the mature retina may follow as a secondary effect of reduced ganglion cell number. This hypothesized effect of ganglion cell number on the generation or survival of inner and outer nuclear layer cells might be relevant to the mechanisms involved in programming different retinal cell densities at different eccentricities.

The essential role of Brn-3b in the development of a subset of retinal ganglion cells and its early appearance during ganglion cell differentiation are reminiscent of the essential role in *C. elegans* of *Unc-86* in a subset of neurons and neuronal precursors and the rapid appearance of *Unc-86* protein within those cells just prior to its time of action (13). These similarities, together with the similarity in sequence between *Unc-86* and the *Brn-3* family, suggest that in the vertebrate CNS the *Brn-3* genes are part of a genetic regulatory circuit that evolved from a simpler *Unc-86*-like system. In this regard, it will be of interest to determine whether targeted mutations in the *Brn-3a* and *Brn-3c* genes produce related or overlapping developmental defects. Finally, the extreme specificity of *Brn-3b* expression and activity suggests that many additional transcriptional regulators exist to control the development of specific subsets of CNS neurons.

The authors thank Mike Delannoy for assistance with plastic embedding and electron microscopy, Drs. Elio Raviola and Sheila Nirenberg for advice on retinal immunocytochemistry, and Drs. King-wai Yau, Randy Reed, and Patrick Tong for helpful comments on the manuscript. This work was supported by the National Eye Institute and the Howard Hughes Medical Institute (J.N.), and by the National Institutes of Health and the Robert Welch Foundation (W.H.K.).

1. Sidman, R. L., Miale, I. L. & Feder, N. (1959) *Exp. Neurol.* **1**, 322–333.
2. Sidman, R. L. (1961) in *The Structure of the Eye*, ed. G. Smelser (Academic, New York), pp. 487–506.
3. Young, R. (1985) *Anat. Rec.* **212**, 199–205.
4. Wässle, H. & Boycott, B. B. (1991) *Physiol. Rev.* **71**, 447–479.
5. Spillman, L. & Werner, J. S. (1990) *Visual Perception: The Neurophysiological Foundations* (Academic, New York).
6. Xiang, M., Zhou, L., Peng, Y.-W., Eddy, R. L., Shows, T. B. & Nathans, J. (1993) *Neuron* **11**, 689–701.
7. Xiang, M., Zhou, L., Macke, J. P., Yoshioka, T., Hendry, S. H. C., Eddy, R. L., Shows, T. B. & Nathans, J. (1995) *J. Neurosci.* **15**, 4762–4785.
8. Gerrero, M. R., McEvilly, R., Turner, E., Lin, C. R., O'Connell, S., Jenne, K. J., Hobbs, M. V. & Rosenfeld, M. G. (1993) *Proc. Natl. Acad. Sci. USA* **90**, 10841–10845.
9. Theil, T., McLean-Hunter, S., Zornig, M. & Moroy, T. (1993) *Nucleic Acids Res.* **21**, 5921–5929.
10. Turner, E. E., Jenne, K. J. & Rosenfeld, M. G. (1994) *Neuron* **12**, 205–218.
11. Finney, M., Ruvkin, G. & Horvitz, H. R. (1988) *Cell* **56**, 757–769.
12. Chalfie, M., Horvitz, H. R. & Sulston, J. E. (1981) *Cell* **24**, 59–69.
13. Finney, M. & Ruvkin, G. (1990) *Cell* **63**, 895–905.
14. Frischauf, A. M., Lehrach, H., Poustka, A. & Murray, N. (1983) *J. Mol. Biol.* **170**, 827–842.
15. McMahon, A. P. & Bradley, A. (1990) *Cell* **62**, 1073–1085.
16. Martinou, J.-C., Dubois-Dauphin, M., Staple, J. K., Rodriguez, I., Frankowski, H., Missotten, M., Albertini, P., Talabot, D., Catsicas, S., Pietra, C. & Huarte, J. (1994) *Neuron* **13**, 1017–1030.
17. LaBossiere, E. & Glickstein, M. (1976) *Histological Processing for the Neural Sciences* (Thomas, Springfield, IL), pp. 39.
18. Sidman, R. L., Angevine, J. B. & Pierce, T. P. (1971) *Atlas of the Mouse Brain and Spinal Cord* (Harvard Univ. Press, Cambridge, MA).
19. Paxinos, G. & Watson, C. (1986) *The Rat Brain in Stereotaxic Coordinates* (Academic, San Diego).
20. Drager, U. C. & Olsen, J. F. (1981) *Invest. Ophthalmol. Visual Sci.* **20**, 285–293.
21. Perry, V. H. (1981) *Neuroscience* **6**, 931–944.
22. Barnstable, C. J. & Drager, U. C. (1984) *Neuroscience* **11**, 847–855.
23. Nixon, R. A., Lewis, S. E., Dahl, D., Marotta, C. A. & Drager, U. C. (1989) *Mol. Brain Res.* **5**, 93–108.
24. Hinds, J. W. & Hinds, P. L. (1974) *Dev. Biol.* **37**, 381–416.
25. McLoon, S. C. & Barnes, R. B. (1989) *J. Neurosci.* **9**, 1424–1432.
26. Wald, D. K. & McLoon, S. C. (1995) *Neuron* **14**, 117–124.
27. Gavrieli, Y., Sherman, Y. & Ben-Sasson, S. A. (1992) *J. Cell Biol.* **119**, 493–501.